7-27-2022

A Simple Parameterization to Enhance the Computational Time in the Three Layer Dry Deposition Model for Smooth Surfaces

Omar M.M. Nofal
The University of Jordan

Omar Al-Jaghbeer
Helsingin Yliopisto

Zaid Bakri
Michigan Technological University, zbakri@mtu.edu

Tareq Hussein
The University of Jordan

Recommended Citation

Nofal, O., Al-Jaghbeer, O., Bakri, Z., & Hussein, T. (2022). A Simple Parameterization to Enhance the Computational Time in the Three Layer Dry Deposition Model for Smooth Surfaces. *Atmosphere, 13*(8). http://doi.org/10.3390/atmos13081190
Retrieved from: https://digitalcommons.mtu.edu/michigantech-p/16394

Follow this and additional works at: https://digitalcommons.mtu.edu/michigantech-p

 Part of the Physics Commons

atmosphere

MDPI

Article

A Simple Parameterization to Enhance the Computational Time in the Three Layer Dry Deposition Model for Smooth Surfaces

Omar M. M. Nofal [1], Omar Al-Jaghbeer [2], Zaid Bakri [3] and Tareq Hussein [1,2,*]

[1] Environmental and Atmospheric Research Laboratory (EARL), Department of Physics, School of Science, The University of Jordan, Amman 11942, Jordan; amr9170120@ju.edu.jo
[2] Institute for Atmospheric and Earth System Research (INAR/Physics), University of Helsinki, FI-00014 Helsinki, Finland; amr8190216@ju.edu.jo
[3] Physics Department and Atmospheric Science Program, Michigan Technological University, Houghton, MI 49931, USA; zbakri@mtu.edu
* Correspondence: tareq.hussein@helsinki.fi

Abstract: Optimization of dry deposition velocity calculation has been of great interest. Every time, determining the value of the concentration boundary layer (CBL) thickness led to a waste of numerical calculation time, which appears as a huge time in large-scale climate models. The goal of this study is to optimize the numerical calculation time in the three-layer deposition model for smooth surfaces through the development of a MATLAB code that can parameterize the appropriate concentration boundary layer height (y^+_{cbl}) and internal integral calculation intervals for each particle diameter D_p (0.01–100 μm) and friction velocity u^* (0.01–100 m/s). The particle concentration, as a solution to the particle flux equation, is obtained and modeled numerically by performing the left Riemann sum using MATLAB software. On the other hand, the number of subdivisions N of the Riemann sum was also parameterized for each D_p and u^* in order to lessen the numerical calculation time. From a numerical point of view, the new parameterizations were tested by several computers; about 78% on the average of the computation time was saved when compared with the original algorithm. In other words, on average, about 1.2 s/calculation was gained, which is valuable in climate models simulations when millions of dry deposition calculations are needed.

Keywords: three-layer deposition model; dry deposition velocity; Brownian diffusion; Eddy diffusion; gravitational settling; concentration boundary layer thickness; parameterization; numerical calculation time; global models; friction velocity

Citation: Nofal, O.M.M.; Al-Jaghbeer, O.; Bakri, Z.; Hussein, T. A Simple Parameterization to Enhance the Computational Time in the Three Layer Dry Deposition Model for Smooth Surfaces. *Atmosphere* **2022**, *13*, 1190. https://doi.org/10.3390/atmos13081190

Academic Editors: Yubin Li and Jie Tang

Received: 21 June 2022
Accepted: 22 July 2022
Published: 27 July 2022

1. Introduction

Particle dry deposition is important in many aspects of applications, such as environmental (atmospheric climate, rooms clean, deposition on vegetation, etc.), industrial (paper industry, copying on papers, painting, ventilation ducts, insecticides, etc.), medical (deposition in pulmonary airway replicas, respiratory tract deposition, aerosol contaminant deposition on human skin, etc.), pharmaceutical (treatment by deposition of pharmaceutical aerosol, etc.), etc. [1–13]. Therefore, accurate estimation of the number of particles being transferred from the airborne state into the deposit state is a vital aspect. The development in the computational part is as important as that in the theoretical or the experimental part in this matter. For example, the computational time required to estimate (or calculate) the deposition velocity of the particle flux towards a surface becomes tremendously long and expensive when the dry deposition is taken into account in global aerosol models. In that sense, parameterizations are introduced to make the computational resources less expensive, i.e., save computational time. In addition to that, parameterization is a valuable method in situations where the details are not apparent or cannot be measured experimentally, as in medical, pharmaceutical, and climate modeling, and is an affordable method in

situations in which the wrong results are expensive, as in industrial applications, so we can use modeling and, as a sequence, parameterizations to test a hypothesis [14].

In general, dry deposition onto a surface is assumed to occur through two major processes. First, advection and turbulent mixing transport the airborne particles to the region adjacent to the deposition surface, reaching the so-called concentration boundary layer (CBL), which is, from a fluid mechanics point of view, a thin layer formed by fluid in the immediate neighborhood of surrounding surface. Second, transport mechanisms transport the particles from the air and deposit them onto the surface. It is believed that the second process controls the particle flux towards the surface when the fluid adjacent to the surface is turbulently well mixed [15]. The major particle transport mechanisms within the CBL include Fickian diffusion (Brownian and Eddy), gravitational settling, and turbophoresis, and the minor mechanisms can be thermophoresis, electrophoresis, magnetophoresis, etc. [16].

The dry deposition velocity (V_d), which is a measure of the effectiveness of the deposition mechanism, is derived from the particle flux equation. It is governed by certain boundary conditions [16–19]. For example, V_d for particles being transported under gravitational settling and under the effect of turbophoresis is dominant for particles with large relaxation time τ_p (i.e., particles with larger mass) [20]. Another example is the influence of the friction velocity (u^*); increasing u^* results in enhancement in V_d for particles with small τ_p (i.e., small particles). In the situations of inhomogeneous air turbulence, increasing u^* can also enhance the deposition of particles with large τ_p because of enhanced turbophoresis.

From a modeling point of view, we are interested in developing more robust models either by enhancing the theory or by introducing new algorithms. With respect to theoretical development, several approaches have been introduced, trying to formulate the best mathematical expressions that can construct the proper model that fits well with the measured data [18,19,21]. However, the lack of understanding of the nature of the CBL parameters (y_0 and y_{cbl}, which are presented in Figure 1) is considered a major challenge. For example, Kallio and Reeks [22] developed a power law expression to achieve a mathematical representation based on a Direct Numerical Simulation (DNS) after Kim et al. [23]. After that, it was assumed that CBL height could be set to 30 (dimensionless units; $y^+{}_{cbl}$) above a smooth surface [18,19]. This height was set to 100 for large particles [15] and 200 for rough surfaces [21]. However, the chosen value for the CBL height (i.e., y_{cbl}) and starting level (i.e., y_0) above the surface area ought to be defined based on the particle concentration profile within the boundary layer. This depends on several factors, including u^*, particle diameter (D_p), and the deposition mechanism.

Here, we introduced a simple parameterization for the y_{cbl} as a function of u^* and D_p. This parameterization was developed for a wide particle size range (D_p 0.01–100 μm) and u^* within the range 0.01–100 m/s. This reflects typical conditions for dry deposition in most physical systems and applications. The parameterization was then implemented in the well-known three-layer dry deposition model in order to improve the computational time required to calculate the dry deposition velocity V_d.

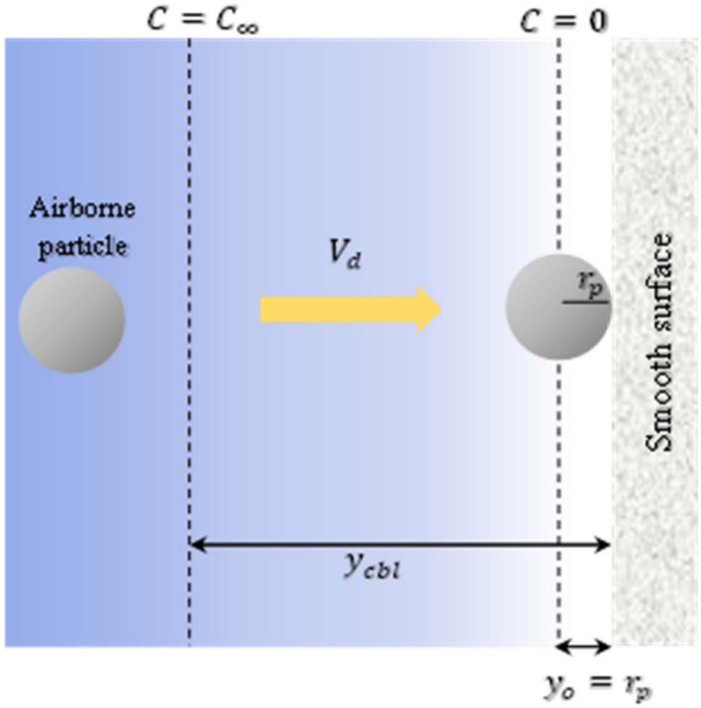

Figure 1. Schematic diagram for dry deposition on a smooth surface of airborne particle with radius r_p across the concentration boundary layer. The concentration of particle number across the boundary layer grows from lowest value ($C = 0$) at height y_0 (= r_p) to its highest value ($C = C_\infty$) at height y_{cbl}. V_d is the dry deposition velocity through the concentration boundary layer.

2. Materials and Methods

2.1. Three-Layer Dry Deposition Model

The mathematical formulation of the well-known three-layer dry deposition model is based on Eulerian approach for the particle flux across the CBL towards the surface [4,15,16,18,19,21,24–31]

$$J = J_{Fickian} + J_{Gravitational} + \sum_n J_n, \quad (1)$$

where J is the total particle flux, $J_{Fickian}$ is the particle flux due to Fickian diffusion (Brownian and Eddy), $J_{Gravitational}$ is the particle flux due to gravitational settling, and the sum represents the particle fluxes due to other mechanisms not included in this part of research. For this equation to be valid, a number of assumptions must be confirmed: steady-state particle flux perpendicular to the surface, the particle concentration gradient exists only very close to the deposition surface (i.e., within the CBL), there are no sources or sinks of particles within the boundary layer, and the surface is a perfect sink for particles.

As illustrated in Figure 1, the particle is considered deposited when its center is at a distance y_0 from the surface (i.e., $y_0 = r_p$); thus, the particle concentration is zero in the fluid right above the surface. The CBL has an upper limit above which particle concentration becomes homogeneous (i.e., $dC/dy = 0$) [27]. This implies that the top of the CBL layer (i.e., y_{cbl}) is set at the maximum concentration (i.e., C_∞). In that sense, the key parameters in accurate estimation for the dry deposition velocity are to have the right value for the height of the concentration boundary layer (i.e., y_{cbl}) and to have a well-behaved profile for the particle concentrations (i.e., C) within the boundary layer.

The particle flux due to Fickian diffusion and gravitational settling is given by

$$J = -\left(\varepsilon_p + D\right)\frac{dC}{dy} - iV_sC \quad (2)$$

where ε_p [m^2s^{-1}] is the turbulent (Eddy) diffusivity coefficient, C [m^{-3}] is the particle concentration, D [m^2s^{-1}] is the Brownian diffusivity, y [m] is the height from the surface, $i = 0, 1, -1$ according to the surface orientations, vertical, horizontal facing up (floor) and horizontal facing down (ceiling), respectively, and V_s [ms^{-1}] is the particle velocity of gravitational settling, which is the constant velocity (terminal) towards the surface [28,29]:

$$V_s = \left[\frac{4}{3}\frac{gD_p(\rho_p - \rho)C_c}{\rho C_D}\right]^{1/2} \tag{3}$$

where g [m s^{-2}] is the gravitational acceleration, D_p [m] is the particle diameter, ρ_p [kg m^{-3}] is the particle density, ρ [kg/m^{-3}] is the gas density, C_D [unitless] is the drag coefficient and C_c [unitless] is the Cunningham slip correction coefficient. The deposition velocity V_d is calculated as

$$V_d = \frac{|J(y=0)|}{C_\infty}, \tag{4}$$

For convenience, the model is described in the dimensionless formulation (Abbreviations)

$$\frac{V_d^+}{D^+} = \frac{dC^+}{dy^+} + \frac{iV_s^+}{D^+}C^+ = \frac{dC^+}{dy^+} + p(y^+)C^+, \tag{5}$$

which has the general solution for the dimensionless particle concentration C^+ as a function of the dimensionless height y^+ [32]

$$C^+ = \frac{1}{F(y^+)}\int_{y_o^+}^{y^+}\frac{V_d^+}{D^+}F(x).dx, \tag{6}$$

$$\frac{1}{V_d^+} = \frac{1}{F(y_{cbl}^+)}\int_{y_o^+}^{y_{cbl}^+}\frac{1}{D^+}F(x).dx, \tag{7}$$

$$F(x) = exp(\int_{y_o^+}^{x} p(y^+).dy^+), \tag{8}$$

$$C^+\big|_{y_0^+ \to r_p^+} = 0 \quad C^+\big|_{y^+ \to y_{cbl}^+} = 1, \tag{9}$$

It is evident that accurate calculation of $y^+{}_o$ and $y^+{}_{cbl}$ leads to accurate calculation for V_d. The determination of the appropriate value of $y^+{}_{cbl}$ for each D_p at a certain u^* will be discussed hereafter.

2.2. Parametrization for $y^+{}_{cbl}$

In the numerical investigation, we treated $y^+{}_{cbl}$ as an unknown quantity to be determined for each particle size and friction velocity. In other words, the upper limit of the integral in Equation (7) was set to $y^+{}_{max}$, which satisfies the second boundary condition in the numerical investigation; when C^+ reaches 1. The method of left Reimann sum was adopted to evaluate the integral using MATLAB^{TM} software (including Simulink toolboxes). It was evaluated by limiting the height from the surface with the parameter $y^+{}_{max}$ to a certain value aiming for the determination of $y^+{}_{cbl}$. The distance from the surface to $y^+{}_{max}$ was divided equally into a proper number of intervals (N) that lead to an accurate solution for V_d.

The numerical investigations were performed for the particle diameter range 0.01–100 µm, friction velocity range 0.01–100 m/s, $y^+{}_{max}$ up to 1000, and N up to 1000 subdivisions for y^+. The $y^+{}_{cbl}$ and N for each parameter varied to obtain convergent solutions for V_d. The variation of $y^+{}_{cbl}$ (0–1000) was performed continuously and repeatedly using a MATLAB^{TM} code that can repeat the solution of Equation (7) until the value of V_d convergent to a certain value; at that end, the code gives us the values of V_d and $y^+{}_{cbl}$ as outputs at a certain friction velocity where N = 1000 at this stage. After we parameterize $y^+{}_{cbl}$ and V_d get known and convergent to non-parameterized value we

proceeding the parameterization for N in order to diminish the calculation time further by using y^+_{cbl} as input and N as variable in this stage until the same V_d achieved.

In the literature, as mentioned above in the introduction, each study case takes a certain value of y^+_{cbl} according to certain assumptions that meet the conditions considered in the model needs. For example, it was assumed to have y^+_{cbl} = 30 for a smooth surface and fine particles [18,19,33]. For micron particles, it was suggested that y^+_{cbl} = 100 [15]. for a rough surface it was suggested that y^+_{cbl} = 200 [21]. Figure 2 illustrates the variation of y^+_{cbl} with D^+_p by using a certain u^* (= 100 m/s) and N (= 1000 subdivisions)

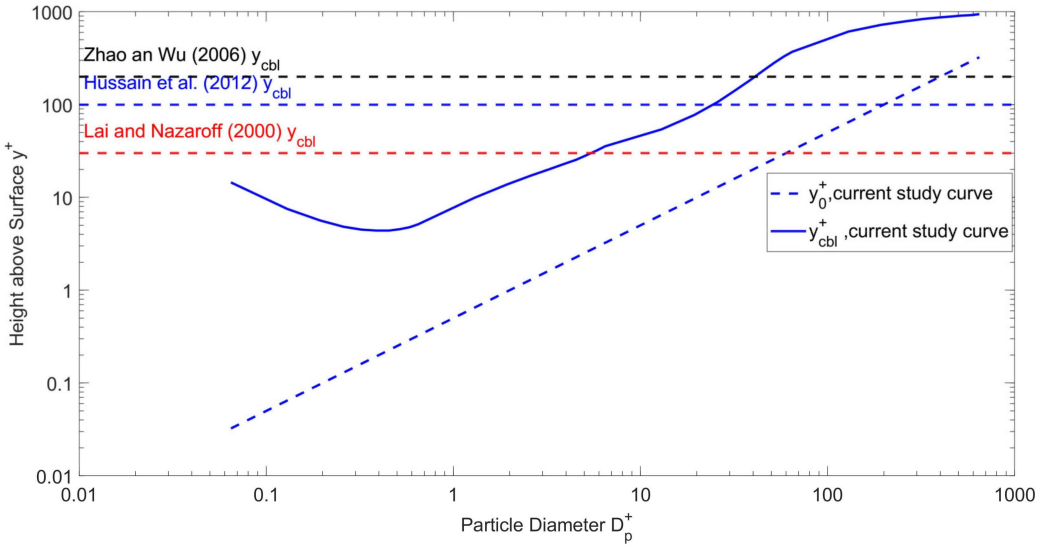

Figure 2. Illustration of the Variation of the concentration boundary layer height above the surface in dimensionless unit (y^+) with the dimensionless particle diameter (D^+_p) for the current study. The horizontal dashed lines resemble the limit value for y^+_{cbl} used in the calculation by Zhao and Wu [19], Hussain et al. [15], and Lai and Nazaroff [18]. Friction velocity u^* = 100 m/s, and number of subdivisions N = 1000 subdivisions.

As will be shown later in the results and discussion and also made evident in Figure 2, one can conclude that if the D^+_p is about 50 and above, none of the previous assumptions for y^+_{cbl} is satisfactory. Furthermore, for D^+_p about 0.3, it is a waste of computational time for calculation to take the y^+_{cbl} larger than 5, so our new parameterizations, as will be shown in the next section, determine a proper y^+_{cbl} and N for each D^+_p at a certain u^*.

We developed two parameterizations. The first one for y^+_{cbl} as a function of D_p and u^*. The second one for N as a function of D_p and u^*. These parameterizations were utilized in the three-layer deposition model so that the most suitable y^+_{cbl} and N are used as pre-set input parameters in the V^+_d calculation. The enhancement in the computational time was then compared between the original algorithm and the new one with these parameterizations.

3. Results and Discussion

3.1. A Parameterization for Fickian Diffusion

In the beginning, the effect of Fickian diffusion (Eddy and Brownian diffusion) was parameterized. In order to investigate the concentration boundary layer height, the y^+_{cbl} parameter, the integral in Equation (7), was evaluated using MATLAB code by taking the height from the surface $y^+_o = r^+_p$ to y^+_{max} = 1000, aiming to determine y^+_{cbl}. The distance from the surface to y^+_{max} was divided equally into a number of subdivisions N = 1000, which leads to an accurate solution for V^+_d. That was calculated for each particle diameter and friction velocity determined in the range mentioned above. Figure 3a shows the y^+_{cbl} profile; from the figure, one can notice the dependence of y^+_{cbl} on the dimensionless particle

relaxation time τ^+_p (or particle size D_p) and u^*. Figure 3b shows the 3-D matrix we obtained for y^+_{cbl} as a function D_p and u^*.

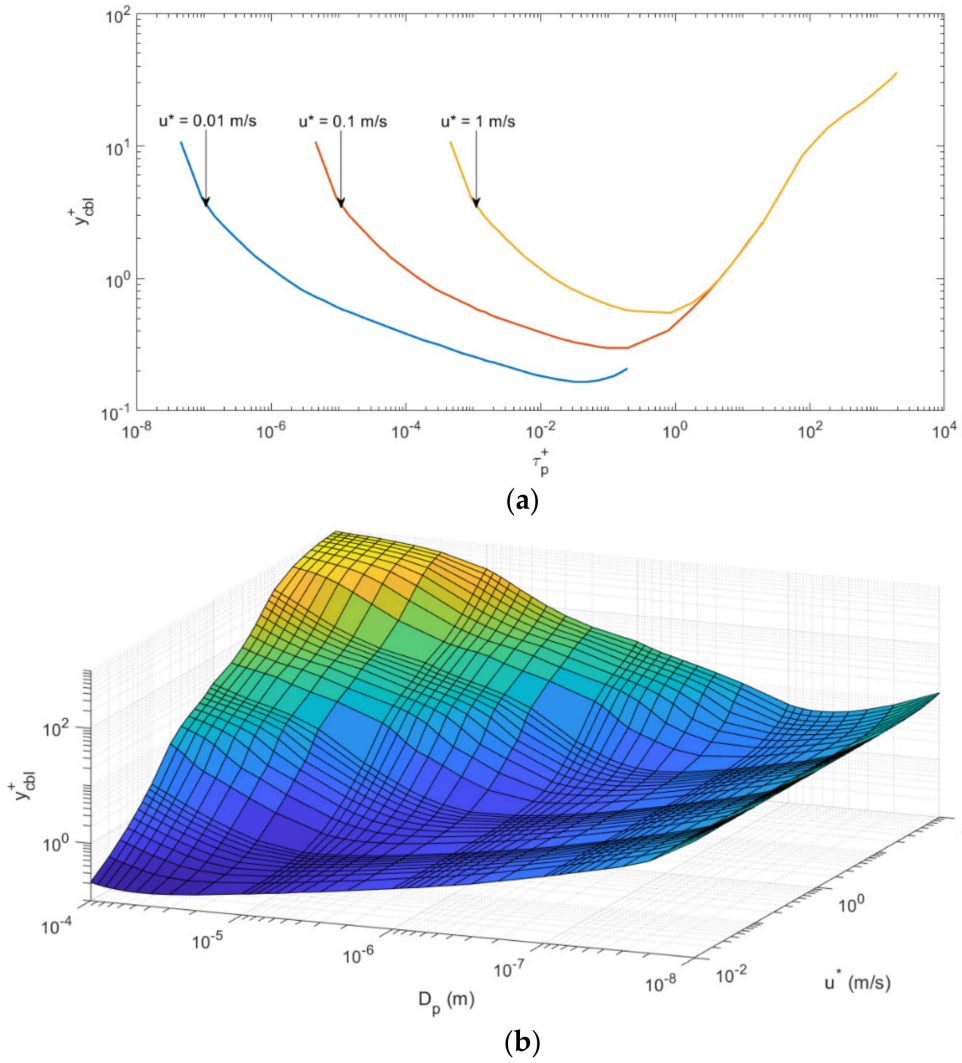

Figure 3. Dependence of y^+_{cbl} on particle size (τ^+_p or D_p) and friction velocity (u^*) for Fickian diffusion: (**a**) profile of y^+_{cbl} as a function of τ^+_p for three friction velocities. (**b**) y^+_{cbl} as a function of D_p (10 nm–100 µm) and u^* (0.01–100 m/s).

From Figure 3b, it seems that the y^+_{cbl} decreases as the D_p increases for small $u^* < 0.02$ m/s, where for 0.02 m/s < u^* < 0.3 m/s the y^+_{cbl} decreases for D_p (<8 μm) and then increases smoothly as D_p increases. For 0.3 m/s < u^* < 10 m/s, the behavior is almost the same, but the y^+_{cbl} decreases for small D_p (<0.3 μm) and then increases steeper than the previous range as D_p increases. Finally, for $u^* > 10$ m/s, the y^+_{cbl} decreases for small D_p (<0.3 μm) and then increases steeply as D_p increases.

In order to get the number of subdivisions N at which the conversion is achieved for the dry deposition velocity (V^+_d) for each particle diameter at a certain friction velocity, we varied N in the code until we obtained the accurate value of V^+_d for each D_p and u^*. The 3-D matrix we obtained for N as a function D_p and u^* is illustrated in Figure 4. The largest N (= 100) is for the smallest D_p and u^* and then decreases (the smallest value is 50) in general as D_p or u^* increases (Figure 4). This behavior has varied for many particle diameters, where N fluctuated for large values of u^* and D_p.

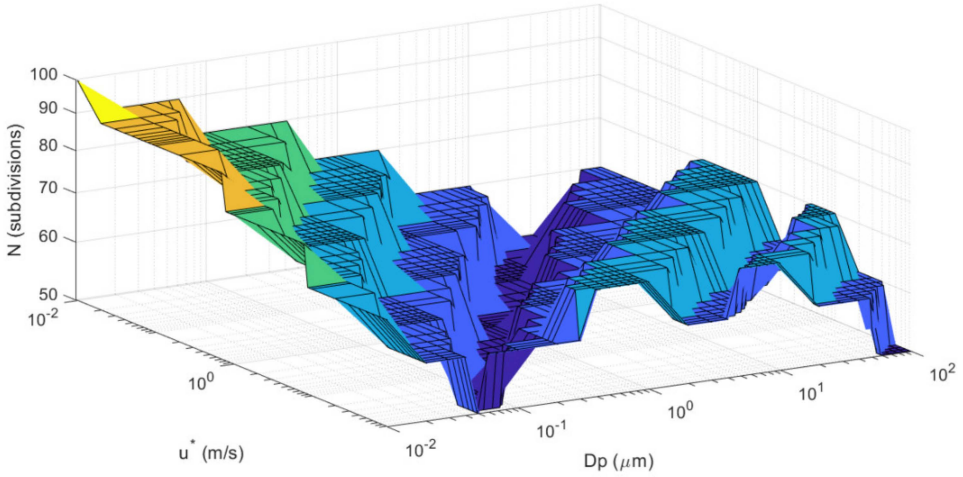

Figure 4. Appropriate number of subdivisions N for each pair of D_p (10 nm–100 μm) and u^* (0.01–100 m/s).

3.2. The Inclusion of Gravitational Settling

In this case, the effect of gravitational settling in addition to the effect of Fickian diffusion was studied. The y^+_{cbl} parameter was investigated by solving the integral in equation (6) was evaluated using MATLAB code and taking the height from the surface with the parameter y^+_{max} = 1000 again. The area under the curve was calculated by partitioning the area to N = 1000 subdivisions, and then the integral was calculated for each D_p and u^* and in the range determined. The profile of the y^+_{cbl} and the 3-D matrices we obtained for y^+_{cbl} as a function D_p and u^* is shown in Figure 5a,b; respectively.

Due to the mixing of two mechanisms, Fickian diffusion, and gravitational settling, the surface obtained in Figure 5b is not as smooth as that of Fickian diffusion alone. Despite the fact that there are some small fluctuations, the general behavior is the same. We notice that the conversion is achieved for V^+_d at the same N for the same D_p and u^* in this case is identical with that of the Fickian diffusion effect alone.

The parameterization was finished after we carried out the 4-D matrix for y^+_{cbl} and N as a function D_p and u^*. At this stage, we transformed to another phase, which is the goal of our study, which was the optimization of calculation time by updating the code to select the appropriate y^+_{cbl} and N based on the input u^* and D_p.

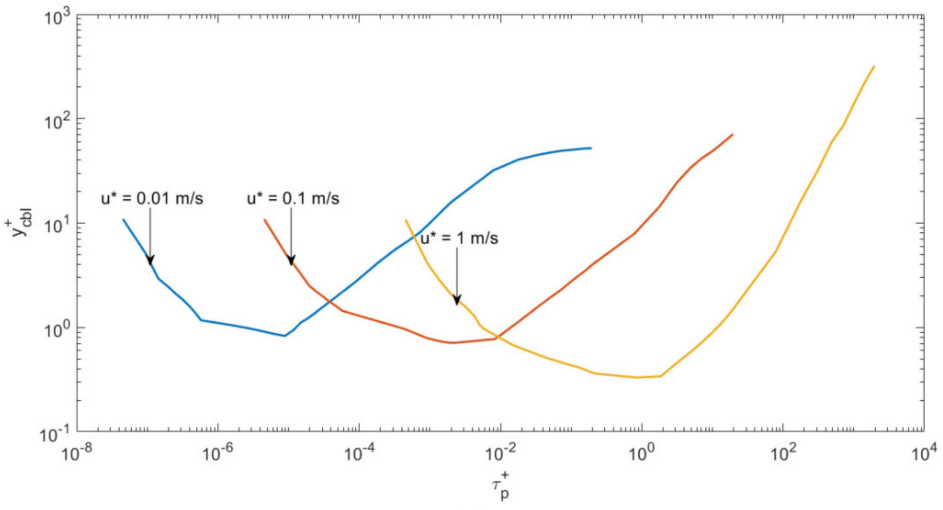

(**a**)

Figure 5. *Cont.*

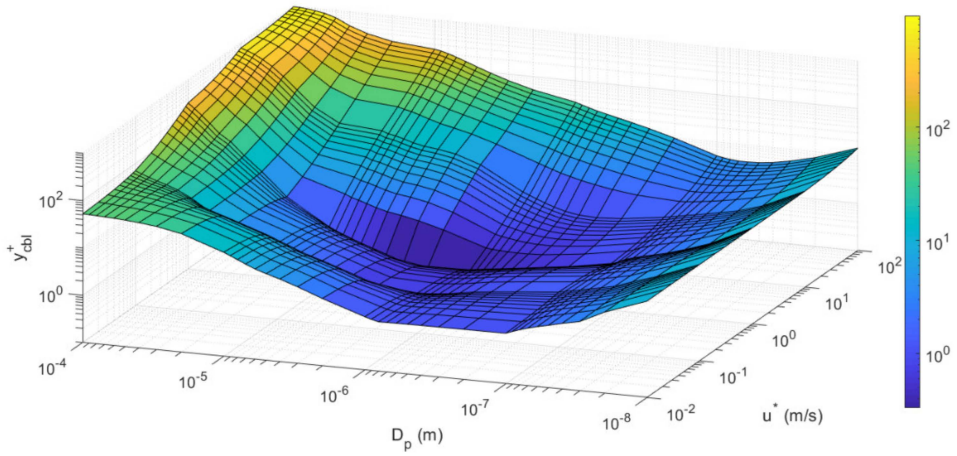

(**b**)

Figure 5. Dependence of y^+_{cbl} on particle size (τ^+_p or D_p) and friction velocity (u^*) when gravitational settling is added to Fickian diffusion: (**a**) profile of y^+_{cbl} as a function of the dimensionless relaxation time τ^+_p for three friction velocities. (**b**) y^+_{cbl} as a function of D_p (10 nm–100 μm) and u^* (0.01–100 m/s).

3.3. Computation Advantage by the Parameterization

To verify the optimization, in the case of Fickian diffusion alone and in the case of Fickian diffusion and gravitational settling together, we utilized the optimized code and the original one in order to make a comparison between them to find V^+_d. The calculations were performed by four computers for the two codes for selected particle diameters for three different friction velocities (u^* = 0.01, 0.1, and 1 m/s). Specifications of computers used for testing running time are summarized in Table 1.

Table 1. Computers specifications.

Computer	Processor (CPU)	Memory (RAM)	Storage
PC-1	Core i7 10th, generation	8 GB	256 SSD
PC-2	Core i5 2nd, generation	4 GB	256 SSD
PC-3	AMD RYZON 3, 3rd generation	4 GB	256 SSD
PC-4	Core i7 3rd, generation	8 GB	250 SSD

Here we compare the time elapsed for each code to obtain the accurate value of V^+_d. To add a flavor to our calculations, we found the time gained as percent time gained (% time) by the percent error method and as the time difference. The results are summarized in Tables 2–4. Notice that Table 2 is for friction velocity u^* = 0.01 m/s, Table 3 is for friction velocity u^* = 0.1 m/s, and Table 4 is for friction velocity u^* = 1 m/s.

Several conclusions can arrive from a deep look at Tables 2–4 details. First, the percent of the average time gained in each part of Table 2, Table 3, and Table 4 and/or each friction velocity (u^* = 0.01, 0.1, and 1 m/s) are 77%, 78%, and 79% respectively. Second, the percent of the average time gained for PC-1 is 79%, for PC-2 is 74%, for PC-3 is 80%, and for PC-4 is 80%. Or in general, the percent of the overall average time gained for all PCs over the range of friction velocities is 78%, which means that we need only 22% of the running time of the original code to run the optimized code. From a computer specification point of view, PC-1 and PC-4 have the same processor, memory (RAM), and storage, but the generation is different, despite that the percent of the average time gained is 79% and 80%, respectively. PC-2 and PC-3 have the same memory (RAM) and storage, but the generation and processor are different, which caused the percent of the average time gained to be 74% and 80%, respectively. From this point of view, we can deduce that processors significantly affect the percent of the average time gained rather than the other computer specifications.

From another point of view, the average time difference for the selected friction velocities for each computer (PC-1, PC-2, PC-3, and PC-4) is about 0.47 s, 1.0 s, 2.0 s, and 1.1, respectively, with a total average for all computers, is about 1.2 s. On the other hand, the average time difference for all computers for each friction velocity (i.e., for each table) is roughly the same, which is about 1.2 s. That means if we need to make just a million calculations by optimized code and saving 1.2 s/calculation, we will save about 280 h out of 356 h (or 11.6 days out of 14.8 days); this simple example opens the imagination to the effectiveness of the optimization in global models' calculation by regular computers instead of super computers. For example, in climate modeling as a global model, if we divide the Earth's surface area (510,072,000 km^2) [34] into a grid whose spatial resolution is 50 km × 50 km or at most 100 km × 100 km, which is relatively high resolution, the computer time on the fastest computers to simulate an experiment along one century may spend several weeks typically due to the large number of calculations required [14]. It seems affordable to use parameterizations that can save about 78% of the computational time (i.e., increasing the computing power), which stimulates us to include more factors that affect the dry deposition and/or use a grid with higher resolution.

Table 2. A comparison between computation time for unoptimized code (without parameterization) and optimized one (with parameterization). for four computers for a selected particle diameters (D_p) for friction velocity u^* = 0.01 m/s.

PC	D_p (μm)	Calculation Time (s) Without Parameterization	Calculation Time (s) With Parameterization	% Time	Time Difference (s)
PC-1	0.01	0.60	0.15	75%	0.45
	0.1	0.67	0.17	75%	0.50
	1	0.63	0.15	76%	0.48
	10	0.61	0.13	78%	0.48
	100	0.56	0.14	74%	0.42
PC-2	0.01	1.6	0.38	76%	1.2
	0.1	1.5	0.40	73%	1.1
	1	1.5	0.38	74%	1.1
	10	1.4	0.37	74%	1.0
	100	1.3	0.36	72%	0.94
PC-3	0.01	2.5	0.52	79%	2.0
	0.1	2.8	0.52	81%	2.3
	1	2.3	0.51	78%	1.8
	10	2.4	0.48	80%	1.9
	100	2.7	0.46	83%	2.2
PC-4	0.01	1.4	0.31	78%	1.1
	0.1	1.4	0.28	80%	1.1
	1	1.3	0.30	77%	1.0
	10	1.3	0.26	80%	1.0
	100	1.3	0.25	80%	1.0

Table 3. A comparison between calculation time for unoptimized code (without parameterization) and optimized one (with parameterization) for four computers for a selected particle diameters (D_p) for friction velocity u^* = 0.1 m/s.

PC	D_p (μm)	Calculation Time (s) Without Parameterization	Calculation Time (s) With Parameterization	% Time	Time Difference (s)
PC-1	0.01	0.70	0.10	86%	0.60
	0.1	0.66	0.15	77%	0.51
	1	0.63	0.13	79%	0.50
	10	0.60	0.13	78%	0.47
	100	0.58	0.13	77%	0.45
PC-2	0.01	1.6	0.40	76%	1.2
	0.1	1.5	0.37	75%	1.1
	1	1.4	0.36	75%	1.0
	10	1.4	0.40	70%	1.0
	100	1.2	0.37	68%	0.8
PC-3	0.01	2.7	0.49	82%	2.2
	0.1	2.2	0.48	78%	1.7
	1	2.4	0.46	81%	1.9
	10	2.2	0.50	78%	1.7
	100	2.7	0.55	79%	2.2
PC-4	0.01	1.5	0.27	81%	1.2
	0.1	1.3	0.25	81%	1.0
	1	1.8	0.24	87%	1.6
	10	1.2	0.30	74%	0.9
	100	1.4	0.26	82%	1.1

Table 4. A comparison between calculation time for unoptimized code (without parameterization) and optimized one (with parameterization) for four computers for a selected particle diameters (D_p) for friction velocity u^* = 1 m/s.

PC	D_p (μm)	Calculation Time (s) Without Parameterization	Calculation Time (s) With Parameterization	% Time	Time Difference (s)
PC-1	0.01	0.68	0.13	81%	0.55
	0.1	0.65	0.13	80%	0.52
	1	0.75	0.13	83%	0.62
	10	0.62	0.13	79%	0.49
	100	0.59	0.13	78%	0.46
PC-2	0.01	1.6	0.41	74%	1.2
	0.1	1.6	0.38	76%	1.2
	1	1.5	0.39	74%	1.1
	10	1.2	0.38	69%	0.82
	100	1.1	0.26	77%	0.84

Table 4. *Cont.*

PC	D_p (μm)	Calculation Time (s) Without Parameterization	With Parameterization	% Time	Time Difference (s)
PC-3	0.01	2.7	0.46	83%	2.2
	0.1	2.4	0.50	79%	1.9
	1	2.6	0.53	80%	2.1
	10	2.4	0.45	81%	2.0
	100	2.3	0.44	81%	1.9
PC-4	0.01	1.2	0.26	78%	0.94
	0.1	1.2	0.24	80%	1.0
	1	1.5	0.26	83%	1.2
	10	1.3	0.30	77%	1.0
	100	1.7	0.26	85%	1.4

Since y^+_{cbl} and N parameters are the factors that affect the running time; the time gained in the case of gravitational settling and Fickian diffusion together is identical to that we obtained for Fickian diffusion alone because N does not change in the two cases, and we use in the optimized code the y^+_{cbl} matrix that shown in Figure 5b since it includes y^+_{cbl} matrix for Fickian diffusion (i.e., we have used just one matrix) in order to shorten the time elapsed for codes to obtain the accurate value of V^+_d.

3.4. The Effect of Parameterization on V^+_d Calculations

Here we compare the values of V^+_d itself before and after optimization. The results we obtained after optimization, which appear as dashed curves, are almost identical to the results we have before optimization, which appear as solid curves, as shown in Figure 6a for Fickian diffusion. This figure implicitly tells us that we gain time by using the optimized code without accuracy loss. We verify that by quantitative comparison between parameterized versus non-parameterized dry deposition velocities shown in Figure 6b, notice that the residuals of the order of magnitude of 10^{-5} and the residual points are distributed around zero, which indicates that the parameterization is valuable from the point of calculation of view since the parameterization will not affect the accuracy of the calculation in any application including climate modeling.

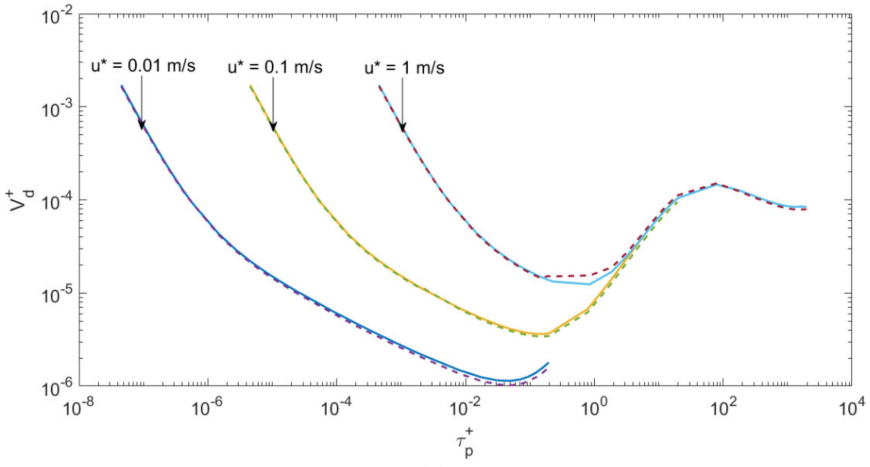

(**a**)

Figure 6. *Cont.*

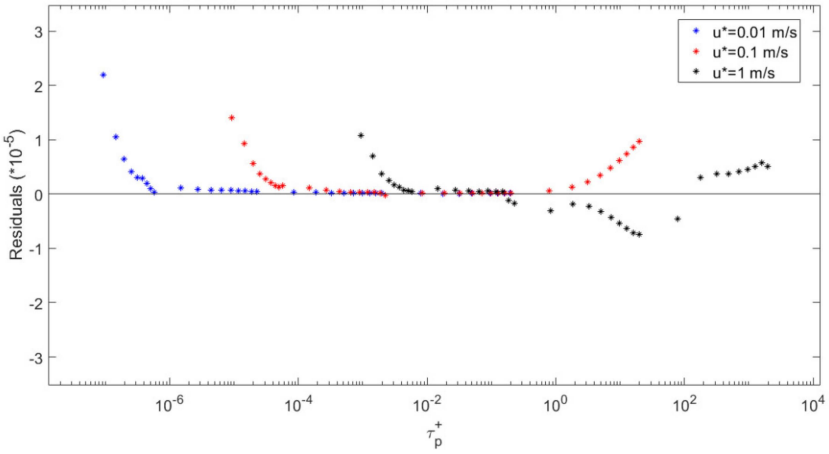

(**b**)

Figure 6. (**a**) A comparison, for Fickian diffusion only, between the optimized code (dashed curves) and the unoptimized code (solid curves) for dry deposition velocity V^+_d. (**b**) the residuals between both codes.

The comparison in the case of gravitational settling and Fickian diffusion together is shown in Figure 7a. It seems that the accuracy is high between the optimized code (dashed curves) and the code we have used before optimization (solid curves). Figure 7b shows the residuals in this case, where it seems that the residuals diverge when the dimensionless particle relaxation time ($\tau^+_p > 0.07$) for small friction velocity ($u^* = 0.01$ m/s) when we take all the residuals into account, and the other residuals point almost lie on residual = 0. In fact, the behavior of residuals, in this case, is selective due to the gravitational settling mechanism.

By magnifying Figure 7b we found that for friction velocity ($u^* = 0.01$ m/s) the divergence appears when $\tau^+_p > 6.46 \times 10^{-6}$ (i.e., $D_p > 0.4$ µm), where the residuals diverge when $\tau^+_p > 8.45 \times 10^{-5}$ (i.e., $D_p > 1$ µm) for friction velocity ($u^* = 0.1$ m/s), and finally the divergence accrue after $\tau^+_p = 7.24 \times 10^{-4}$ (i.e., $D_p > 5$ µm) for friction velocity ($u^* = 1$ m/s), as shown in Figure 7c. These details led us to conclude that our parameterizations, in the case of gravitational settling mechanism is included, are excellent in the case of sub-micron (i.e., fine and ultrafine) particles, whereas in the case of super-micron particles (1 µm < D_p < 10 µm) the parameterizations are excellent for $u^* \geq 1$ m/s since the residuals of an order of magnitude 10^{-5} and the residual points surrounding the residual is zero.

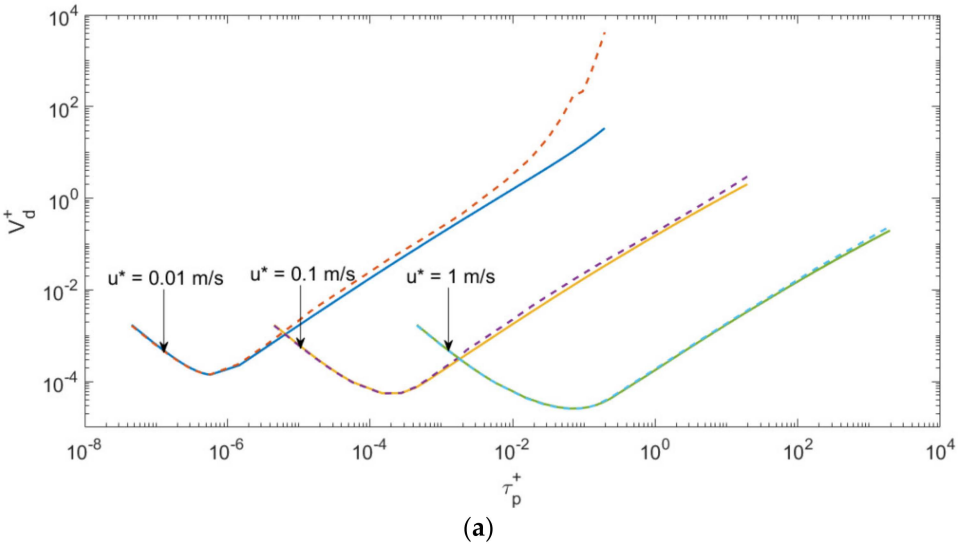

(**a**)

Figure 7. *Cont.*

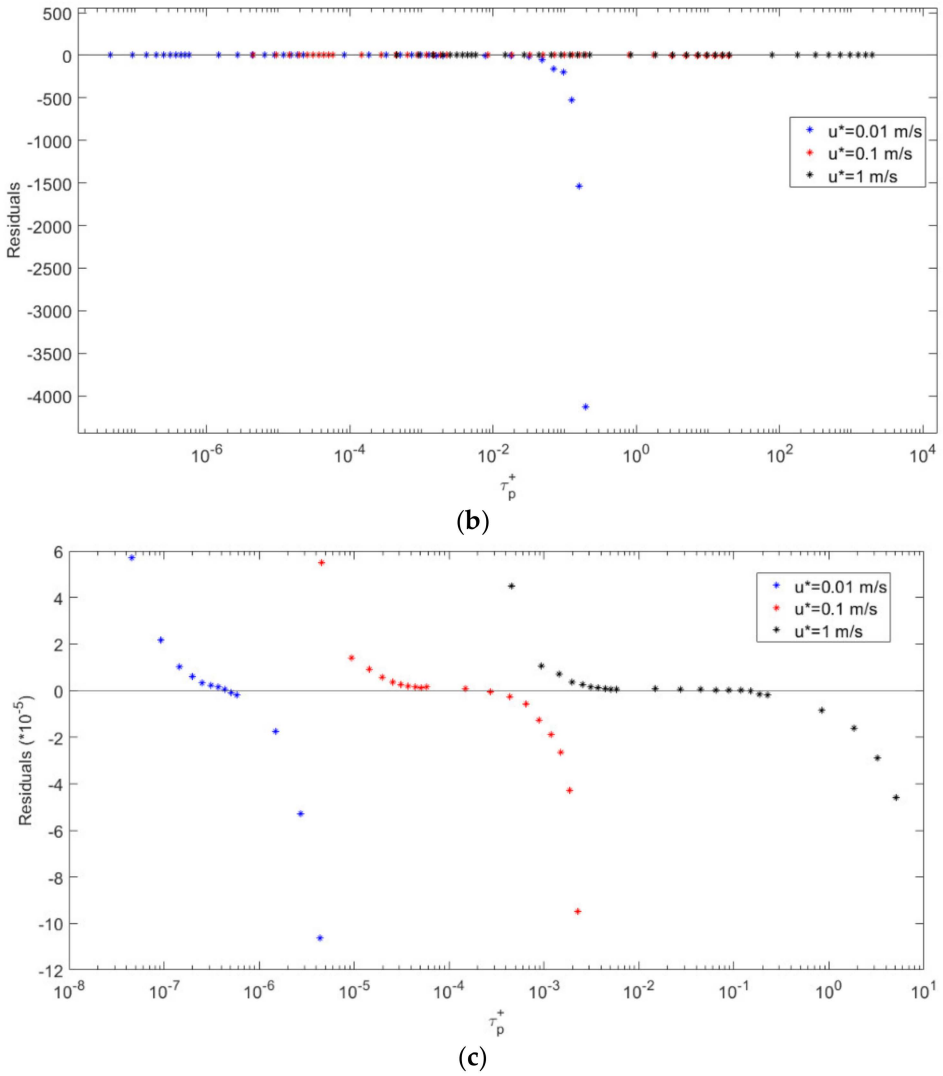

Figure 7. (**a**) A comparison, for gravitational settling and Fickian diffusion together, between the optimized code (dashed curves) and the unoptimized code (solid curves) for dry deposition velocity V^+_d. (**b**–**c**) the residuals between both codes.

Depending on Figures 6 and 7, the differences between non-parameterized and parameterized V^+_d will not affect the accuracy of any calculations, including V^+_d in the climate models and other applications.

4. Conclusions

The present article presented a parameterization to optimize the calculation time for the dry deposition velocity in the three-layer deposition model. That was based on determining a proper concentration boundary layer thickness (y^+_{cbl}) that gives accurate dry deposition velocity (V^+_d) above a smooth surface in a shorter calculation time according to the particle's diameter (D_p) and the friction velocity (u^*).

The formulation of the three-layer deposition model was used in the manipulation of Fickian (Eddy and Brownian) diffusion and gravitational settling mechanisms since they are the dominant mechanisms for small and large particles, respectively.

The solution to the particle flux (J) equation, which is the particle concentration within the boundary layer, was performed by the Riemann sum, so we found a suitable number of subdivisions (N) at which the conversion was achieved for each case along D_p range (10 nm–100 µm) and u^* range (0.01–100 m/s) in addition to the y^+_{cbl}.

After we obtained the optimization parameterization matrix, we plugged it into a MATLAB code of the three-layer deposition model that can pick up or interpolate a convenient value of y^+_{cbl} and N depending on D_p and u^* as the first step of the calculation. This procedure saved up to 78% (average) for each calculation when compared to the time taken for the same code without parameterization, where the comparison was by four computers that have different specifications. In other words, on average, 1.2 s/calculation can be saved, which means that our parameterization can lessen the accumulated time in the case of big data calculations in large-scale climate models.

The verification of our development was performed by comparing the V^+_d we obtained without parameterization with that we obtained with parameterization. The results confirm that the accuracy did not affect the results for the dry deposition calculation value, but the calculation time gain is valuable.

The inclusion of the minor mechanisms, such as turbophoresis, thermophoresis, electrophoresis, magnetophoresis, etc., in addition to the effect of other factors, such as temperature and pressure, on the calculation time is our future work.

Author Contributions: Conceptualization, T.H., O.M.M.N., O.A.-J. and Z.B.; methodology, T.H., O.M.M.N., O.A.-J. and Z.B.; software, O.M.M.N., O.A.-J. and Z.B.; validation, O.M.M.N.; formal analysis, O.M.M.N. and O.A.-J.; investigation, T.H., O.A.-J. and O.M.M.N.; resources, T.H.; data curation, O.M.M.N. and O.A.-J.; writing—original draft preparation, T.H., O.M.M.N., O.A.-J. and Z.B.; writing—review and editing, T.H., O.M.M.N., O.A.-J. and Z.B.; visualization, O.M.M.N. and O.A.-J.; supervision, T.H.; project administration, T.H.; funding acquisition, T.H. All authors have read and agreed to the published version of the manuscript.

Funding: This research was supported by the Deanship of Scientific Research (DSR) at the University of Jordan.

Institutional Review Board Statement: Not applicable.

Informed Consent Statement: Not applicable.

Data Availability Statement: Not applicable.

Acknowledgments: The authors acknowledge the support of the Deanship of Scientific Research (DSR) at the University of Jordan. T.H. acknowledges the support of the Atmosphere and Climate Competence Center (ACCC) Flagship funded by the Academy of Finland (grant# 337549); and the Eastern Mediterranean and Middle East Climate and Atmosphere Research (EMME-CARE) project, which received funding from the European Union's Horizon 2020 Research and Innovation Programme (Grant Agreement Number 856612) and the Government of Cyprus. The sole responsibility of this publication lies with the authors. Open access funding was provided by the University of Helsinki.

Conflicts of Interest: The authors declare no conflict of interest.

Abbreviations

Symbol	Unit	Description
C	m^{-3}	Particle concentration within the boundary layer. In dimensionless form $C^+ = C/C_\infty$ C_∞ is the particle concentration above the boundary layer or far away from the surface
C_c	–	Cunningham slip correction coefficient
D	$m^2\ s^{-1}$	Brownian diffusivity of the particle, $D = k_B\ T\ Cc/3\pi\mu\ D_p$ in dimensionless form $D^+ = (\varepsilon_p + D)/\nu$
D_p	m	Particle diameter, in dimensionless form $D^+_p = D_p\ u^*/\nu$
J	$m^{-2}\ s^{-1}$	Total particle flux across the concentration boundary layer towards the surface. $J_{Fickian}$ is particle flux due to Brownian and Eddy diffusions. J_n is the particle flux across the concentration boundary layer due to other mechanisms to be included in the model in the future

k_B	Joule/K	Boltzmann constant
m_p	kg	Particle mass
r_p	m	Particle radius, in dimensionless form $r^+{}_p = r_p\ u^*/\nu$
T	K	Absolute temperature
u^*	m s^{-1}	Friction velocity
V_d	m s^{-1}	Deposition velocity onto a surface, in dimensionless form $V^+{}_d = V_d/u^*$
$\left\langle V'^2_y \right\rangle$	m^2 s^{-2}	Air wall normal fluctuating velocity intensity, in dimensionless [16,22]: $\left\langle V'^2_y \right\rangle^+ = \frac{\left\langle V'^2_y \right\rangle}{(u*)^2} = \left[\frac{0.005(y^+)^2}{1+0.002923(y^+)^{2.128}}\right]^2$
$\left\langle V'^2_{py} \right\rangle$	m^2 s^{-2}	Particle wall normal fluctuating velocity intensity [31]: $\left\langle V'^2_{py} \right\rangle = \left\langle V'^2_y \right\rangle \left[1+\frac{\tau_p}{\tau_L}\right]^{-1}$ $\left\langle V'^2_{py} \right\rangle^+ = \left\langle V'^2_{py} \right\rangle/(u*)^2$
y	m	Vertical distance from the surface, in dimensionless form $y^+ = y\ u^*/\nu$
y_0	m	Distance from the surface at which the particle with a radius r_p is deposited, in dimensionless form $y^+{}_o = y_0\ u^*/\nu$
y_{cbl}	m	Depth of the concentration boundary layer above which $dC/dy = 0$ in dimensionless form $y^+{}_{cbl} = y_{cbl}\ u^*/\nu$
μ	kg m^{-1} s^{-1}	Dynamic viscosity of the fluid
ρ	kg m^{-3}	Fluid density
τ_L	s	Lagrangian time-scale of the fluid [31]: $\tau_L = \nu_t/\left\langle V'^2_y \right\rangle$ $\tau_L^+ = \tau_L(u*)^2/\nu$
τ_p	s	Particle relaxation time $\tau_p = m_p C_c/3\pi\mu D_p$ $\tau_p^+ = \tau_p(u*)^2/\nu$
ε_p	m^2 s^{-1}	Eddy diffusivity of the particle. For relatively small particles and homogeneous isotropic turbulence [18] $\varepsilon_p = \nu_t$ For any particle size [21,29] $\varepsilon_p = \left[1+\frac{\tau_p}{\tau_L}\right]^{-1}\nu_t$
ν	m^2 s^{-1}	Kinematic viscosity of the fluid, $\nu = \mu/\rho$
$\nu\tau$	m^2 s^{-1}	Air turbulent viscosity. For smooth surfaces it is [17] $\frac{\nu_t}{\nu} = \begin{cases} 7.67\times10^{-4}(y^+)^3, & 0 \le y^+ \le 4.3 \\ 10^{-3}(y^+)^{2.8214}, & 4.3 \le y^+ \le 12.5 \\ 1.07\times10^{-2}(y^+)^{1.8895}, & 12.5 \le y^+ \le 30 \end{cases}$ and for rough surfaces it is [16] $\frac{\nu_t}{\nu} = \begin{cases} \left(\frac{y^+}{11.15}\right)^3, & 0 \le y^+ \le 3 \\ \left(\frac{y^+}{11.4}\right)^3 - 0.049774, & 3 \le y^+ \le 52.108 \\ 0.4y^+, & 52.108 \le y^+ \end{cases}$

References

1. Bozlaker, A.; Muezzinoglu, A.; Odabasi, M. Atmospheric concentrations, dry deposition and air-soil exchange of polycyclic aromatic hydrocarbons (PAHs) in an industrial region in Turkey. *J. Hazard Mater.* **2008**, *153*, 1093–1102. [CrossRef] [PubMed]
2. El-Batsh, H. Modelling Particle Deposition on Compressor and Turbine Blades. Ph.D. Thesis, Vienna University of Technology, Vienna, Austria, 2001.
3. Liu, B.Y.H.; Ahn, K.H. Particle Deposition on Semiconductor Wafers. *Aerosol Sci. Technol.* **1987**, *6*, 215–224. [CrossRef]
4. Lobo, P.; Durdina, L.; Brem, B.T.; Crayford, A.P.; Johnson, M.P.; Smallwood, G.J.; Siegerist, F.; Williams, P.I.; Black, E.A.; Llamedo, A.; et al. Comparison of Standardized Sampling and Measurement Reference Systems for Aircraft Engine Non-Volatile Particulate Matter Emissions. *J. Aerosol Sci.* **2020**, *145*, 105557. [CrossRef]
5. Pui, D.Y.H.; Ye, Y.; Liu, B.Y.H. Experimental Study of Particle Deposition on Semiconductor Wafers. *Aerosol Sci. Technol.* **1990**, *12*, 795–804. [CrossRef]
6. Song, L.; Elimelech, M. Particle Deposition onto a Permeable Surface in Laminar Flow. *J. Colloid Interface Sci.* **1995**, *173*, 165–180. [CrossRef]
7. Tong, X.; Dong, J.; Shang, Y.; Inthavong, K.; Tu, J. Effects of Nasal Drug Delivery Device and Its Orientation on Sprayed Particle Deposition in a Realistic Human Nasal Cavity. *Comput. Biol. Med.* **2016**, *77*, 40–48. [CrossRef] [PubMed]

8. Tong, Z.X.; Li, M.J.; He, Y.L.; Tan, H.Z. Simulation of Real Time Particle Deposition and Removal Processes on Tubes by Coupled Numerical Method. *Appl. Energy* **2017**, *185*, 2181–2193. [CrossRef]
9. Andersson, K.G.; Roed, J.; Byrne, M.A.; Hession, H. Deposition of contaminant aerosol on human skin. *J. Environ. Radioact.* **2006**, *85*, 182–195. [CrossRef]
10. Casal, J.; Planas-Cuchi, E.; Moreso, J.M.; Casal, J. Forecasting virus atmospherical dispersion. Studies with foot-and-mouth disease. *J. Hazard. Mater.* **1995**, *43*, 229–244. [CrossRef]
11. Karlsson, E.; Huber, U. Influence of desorption on the indoor concentration of toxic gases. *J. Hazard. Mater.* **1996**, *49*, 15–27. [CrossRef]
12. Kleinstreuer, C.; Zhang, Z.; Li, Z. Modeling airflow and particle transport/deposition in pulmonary airways. *Respir. Physiol. Neurobiol.* **2008**, *163*, 128–138. [CrossRef] [PubMed]
13. Londah, J.; Pagels, J.; Swietlicki, E.; Zhou, J.; Ketzel, M.; Massling, A.; Bohgard, M. A set-up for field studies of respiratory tract deposition of fine and ultrafine particles in humans. *J. Aerosol Sci.* **2006**, *37*, 1152–1163. [CrossRef]
14. Goosse, H.; Barriat, P.Y.; Lefebvre, W.; Loutre, M.F.; Zunz, V. Introduction to Climate Dynamics and Climate Modeling. Online Textbook. Available online: http://www.climate.be/textbook (accessed on 17 July 2022).
15. Hussein, T.; Smolik, J.; Kerminen, V.M.; Kulmala, M. Modeling Dry Deposition of Aerosol Particles onto Rough Surfaces. *Aerosol Sci. Technol.* **2012**, *46*, 44–59. [CrossRef]
16. Guha, A. A Unified Eulerian Theory of Turbulent Deposition to Smooth and Rough Surfaces. *J. Aerosol Sci.* **1997**, *28*, 1517–1537. [CrossRef]
17. Corner, J.; Pendlebury, E.D. The Coagulation and Deposition of a Stirred Aerosol. *Proc. Phys. Soc. Sect. B* **1951**, *64*, 645–654. [CrossRef]
18. Lai, A.C.K.; Nazaroff, W.W. Modeling Indoor Particle Deposition from Turbulent Flow onto Smooth Surfaces. *J. Aerosol Sci.* **2000**, *31*, 463–476. [CrossRef]
19. Zhao, B.; Wu, J. Modeling Particle Deposition from Fully Developed Turbulent Flow in Ventilation Duct. *Atmos. Environ.* **2006**, *40*, 457–466. [CrossRef]
20. Hussein, T.; Ibrahim, S.; Malek, S. Basic Concepts and Development of Dry Deposition Modelling. *Jordan J. Phys.* **2019**, *12*, 113–132.
21. Zhao, B.; Wu, J. Modeling Particle Deposition onto Rough Walls in Ventilation Duct. *Atmos. Environ.* **2006**, *40*, 6918–6927. [CrossRef]
22. Kallio, G.A.; Reeks, M.W. A Numerical Simulation of Particle Deposition in Turbulent Boundary Layers. *Int. J. Multiph. Flow* **1989**, *15*, 433–446. [CrossRef]
23. Kim, J.; Moin, P.; Moser, R. Turbulence Statistics in Fully Developed Channel Flow at Low Reynolds Number. *J. Fluid Mech.* **1987**, *177*, 133–166. [CrossRef]
24. Crump, J.G.; Flagan, R.C.; Seinfeld, J.H. Particle Wall Loss Rates in Vessels. *Aerosol Sci. Technol.* **1982**, *2*, 303–309. [CrossRef]
25. McMurry, P.H.; Rader, D.J. Aerosol Wall Losses in Electrically Charged Chambers. *Aerosol Sci. Technol.* **1985**, *4*, 249–268. [CrossRef]
26. Nazaroff, W.W.; Cass, G.R. Mathematical Modeling of Indoor Aerosol Dynamics. *Environ. Sci. Technol.* **1984**, *23*, 157–166. [CrossRef]
27. Bejan, A. *Convection Heat Transfer*, 2nd ed.; John Wiley & Sons: New York, NY, USA, 1995.
28. Seinfeld, J.H.; Pandis, S.N. *Atmospheric Chemistry and Physics: From Air Pollution to Climate Change*, 3rd ed.; John Wiley & Sons: New York, NY, USA, 1998.
29. Hinze, J.O. *Turbulence*, 2nd ed.; McGraw-Hill: New York, NY, USA, 1975.
30. Hinds, W.C. *Aerosol Technology*, 2nd ed.; John Wiley & Sons: New York, NY, USA, 1999.
31. Johansen, S.T. The Deposition of Particles on Vertical Walls. *Int. J. Multiph. Flow* **1991**, *17*, 355–376. [CrossRef]
32. Boyce, W.E.; DiPrima, R.C. *Elementary Differential Equations and Boundary Value Problems*, 10th ed.; John Wiley & Sons: New York, NY, USA, 2012.
33. Piskunov, V.N. Parameterization of Aerosol Dry Deposition Velocities onto Smooth and Rough Surfaces. *J. Aerosol Sci.* **2009**, *40*, 664–679. [CrossRef]
34. Pidwirny, M. *Surface Area of Our Planet Covered by Oceans and Continents*; University of British Columbia: Kelowna, BC, Canada, 2006.